Cluster Compounds

$[SiAu_4]$: Aurosilane**

*Boggavarapu Kiran, Xi Li, Hua-Jin Zhai, Li-Feng Cui, and Lai-Sheng Wang**

Because of the strong relativistic effects, the chemistry of gold differs substantially from the rest of the coinage metals.[1–6] The relativistic stabilization of the 6s orbital in gold gives rise to an anomalously high electron affinity of Au, which has been compared to the halogens,[5,7,8] such as in the recently predicted tetraaurides $[MAu_4]$ (M = Ti, Zr, Th).[9] The most remarkable chemistry of gold is the isolobal analogy between a gold phosphane unit $\{AuPR_3\}$ and a hydrogen atom,[10–12] which has been exploited to bring out tetra- and hypercoordination in compounds, such as $[C(AuPR_3)_4]$and $[C(AuPR_3)_5]^+$.[13–17] Herein we show that a single gold atom can also exhibit chemistry analogous to the hydrogen atom. We report experimental and theoretical evidence that a series of Si–Au clusters, $[SiAu_n]$ (n = 2–4), are structurally and electronically similar to SiH_n. Photoelectron spectroscopy (PES) of the corresponding $[SiAu_n]^-$ anions reveals that $[SiAu_4]$ has a large energy gap of 2.4 eV, thus indicating an extremely chemically stable molecule. Ab initio calculations show that $[SiAu_4]$ has an ideal tetrahedral structure and the nature of the chemical bonding in $[SiAu_n]$ has a one-to-one correspondence to that in SiH_n. The chemical stability of the aurosilane, $[SiAu_4]$, suggests that it may be synthesized as an isolated compound. The current finding is also relevant to understanding the chemical interactions in the technologically important silicon–gold interface.

The silicon–gold clusters were produced by laser vaporization of a mixed Au–Si target and their electronic structures were studied by PES (see Experimental Section). Figure 1 shows the PES spectra of $[SiAu_n]^-$ (n = 2–4) at two different photon energies. Numerous transitions were observed for each species. The spectra of $[SiAu_3]^-$ were very broad and the first band seemed to contain two components, a sharp peak overlapping with a more diffused band (Figure 1 d). The most interesting observation was the extremely large energy gap observed in the spectra of $[SiAu_4]^-$ (Figure 1 e,f). This observation suggested that $SiAu_4$ is a highly stable neutral molecule with a large gap between its highest occupied molecular orbital (HOMO) and its lowest unoccupied molecular orbital (LUMO), 2.36 eV as measured by the binding energy difference between the X and A bands (Figure 1 f). The inset of Figure 1 f shows a high resolution spectrum of the X band of $SiAu_4^-$ at 532 nm, revealing a partially resolved vibrational progression with an average spacing of $140 \pm 30\ cm^{-1}$. This observation suggested that both $[SiAu_4]$ and $[SiAu_4]^-$ must be highly symmetric and there is little geometry change between their ground states. The spectra of $[SiAu_2]^-$ also showed a sizable energy gap (1.76 eV), indicating that $SiAu_2$ is a closed-shell molecule. However, we found that the numerous sharp peaks (labeled X′) in the higher binding-energy side (Figure 1 a) were due to contamination of $[Si_8Au]^-$, as a result of a near mass degeneracy between seven Si atoms (mass 196) and one Au atom (mass 197). The adiabatic detachment energies (ADEs) and vertical detachment energies (VDEs) for the first two bands (X and A) for each species are given in Table 1. The sharp X band in the spectra of $[SiAu_2]^-$ and $[SiAu_4]^-$ allowed accurate ADEs to be determined. However, we were only able to estimate a detachment threshold for the X band of $[SiAu_3]^-$ due to its diffused nature.

It has been demonstrated previously that PES combined with ab initio calculations is a powerful tool for elucidating

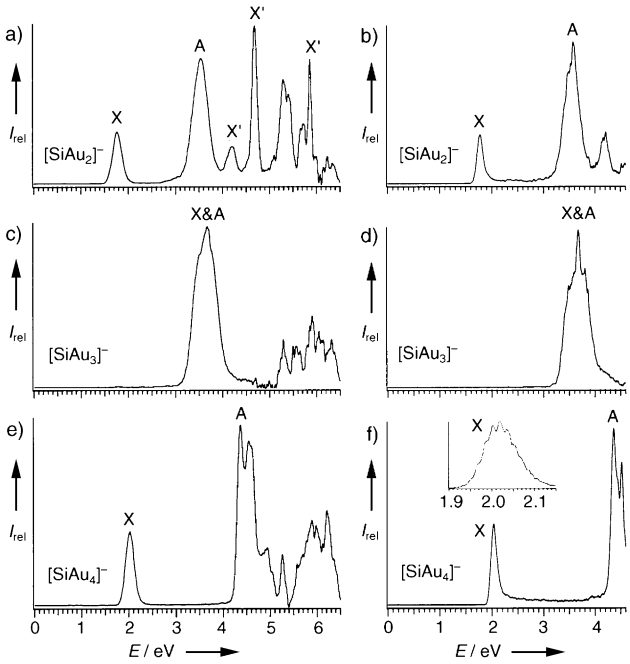

Figure 1. Photoelectron Spectra of $[SiAu_n]^-$ (n = 2–4). a) $[SiAu_2]^-$ at 193 nm (6.424 eV). b) $[SiAu_2]^-$ at 266 nm (4.661 eV). c) $[SiAu_3]^-$ at 193 nm. d) $[SiAu_3]^-$ at 266 nm. e) $[SiAu_4]^-$ at 193 nm. f) $[SiAu_4]^-$ at 266 nm. The inset shows the spectrum taken at 532 nm.

[*] Dr. B. Kiran, X. Li, Dr. H.-J. Zhai, L.-F. Cui, Prof. Dr. L.-S. Wang
Department of Physics
Washington State University
2710 University Drive, Richland, WA 99352 (USA)
and
W. R. Wiley Environmental Molecular Sciences Laboratory
Pacific Northwest National Laboratory
MS K8-88, P.O. Box 999, Richland, WA 99352 (USA)
Fax: (+1) 509-376-6066
E-mail: ls.wang@pnl.gov

[**] Valuable discussions with Dr. Jun Li and Prof. A. I. Boldyrev are gratefully acknowledged. This work was supported by the US National Science Foundation (CHE-0349426) and partly by the Petroleum Research Fund of the American Chemical Society, and performed at the W. R. Wiley Environmental Molecular Sciences Laboratory, a national scientific user facility sponsored by the US Department of Energy's Office of Biological and Environmental Research and located at Pacific Northwest National Laboratory, operated for DOE by Battelle. Part of the calculations was performed with supercomputers at the EMSL Molecular Science Computing Facility.

Supporting information for this article is available on the WWW under http://www.angewandte.org or from the author.

 DOI: 10.1002/anie.200353602

Table 1: Experimental adiabatic (ADE) and vertical (VDE) detachment energies of $SiAu_n^-$ ($n=2$–4) compared to those calculated from the lowest energy isomers. All energies are in eV.

		Experimental		Theoretical: DFT (CCSD(T))[a]	
		ADE	VDE	ADE	VDE
$[SiAu_2]^-$	X	1.68 ± 0.03	1.72 ± 0.03	1.77 (1.67)	1.81 (1.71)
	A		3.48 ± 0.05		3.19
$[SiAu_3]^-$	X	3.22 ± 0.03[b]	3.48 ± 0.02	2.74 (2.93)	3.22 (3.46)
	A		3.67 ± 0.06		3.66
$[SiAu_4]^-$	X	1.96 ± 0.02	2.00 ± 0.01	2.08 (1.79)	2.15 (1.84)
	A		4.36 ± 0.02		4.23

[a] DFT calculations by using hybrid B3-LYP functional and CCSD(T) values are given in parentheses. Aug-cc-pVTZ basis set for Si and Stuttgart 19-electron effective core potentials augmented with two f (0.498 and 1.461) polarization functions were used for both R(U)B3-LYP and R(U)CCSD(T) calculations. [b] Estimated detachment threshold.

the electronic structure and chemical bonding of novel clusters. Inclusion of relativistic and correlation effects are essential to produce accurate structures and energies for gold-containing molecules. We studied the Si–Au clusters by using hybrid density functional theory (DFT) method with effective core potentials, which has been shown previously to be suitable for clusters that involve Au.[18,19] Further refinement was obtained at the coupled-cluster level [CCSD(T)], which incorporates dispersion effects omitted by the DFT methods (see Experimental Section). The two lowest-energy structures for $[SiAu_n]$ and $[SiAu_n]^-$ ($n=2$–4) are given in Figure 2, along with important geometrical parameters.

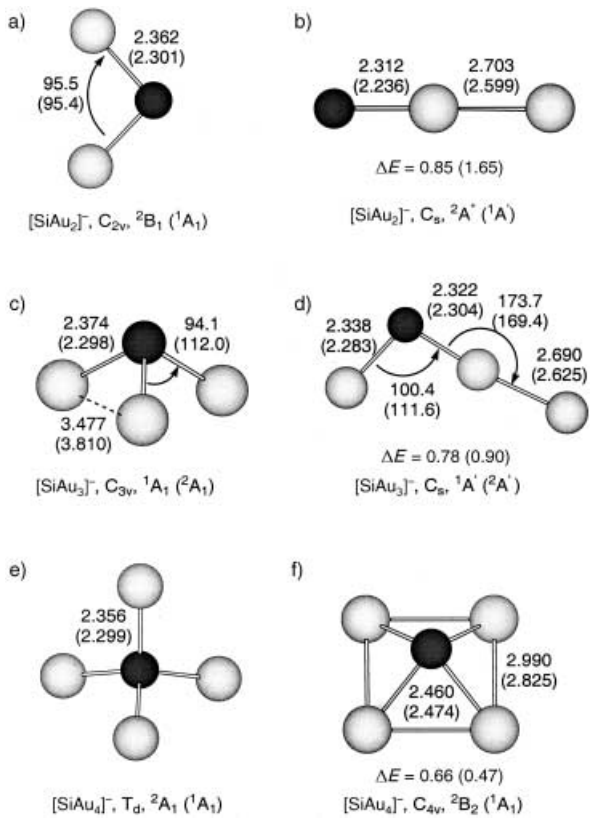

Figure 2. Optimized structures at B3-LYP level for the two low-lying isomers of $[SiAu_n]^-$ and $[SiAu_n]$. All bond lengths are given in angstroms and angles in degrees. The relative energies (in bold) are in eV for the higher energy isomer. The values and the symmetry labels given in the parentheses correspond to the neutral structures.

At all levels of theory, the most stable $[SiAu_2]^-$ structure has C_{2v} symmetry with a doublet $^2B_1$ state (Figure 2a). A quasi-linear C_s isomer (Figure 2b) is much higher in energy. The most stable neutral $[SiAu_2]$ is $^1A_1$ of C_{2v} symmetry with a very similar structure as the anion. The most stable structure of $[SiAu_3]^-$ has C_{3v} symmetry (Figure 2c). The second-lowest isomer (Figure 2d) is 0.78 eV higher in energy. The D_{3h} isomer, which is a transition state (a first-order saddle point) for the umbrella inversion of the C_{3v} $[SiAu_3]^-$, is 0.96 eV higher in energy. The ground state of $[SiAu_3]$ has the same C_{3v} symmetry as the anion, but there is a large geometry change upon electron detachment. The Si–Au bond length is decreased by 0.07 Å and the ∢SiAuSi bond angle increased considerably by 18° in $[SiAu_3]$ relative to $[SiAu_3]^-$ (Figure 2c). For $[SiAu_4]^-$, we calculated several isomers and found the most stable structure is tetrahedral (Figure 2e) with a pyramidal low-lying isomer (Figure 2f) at both the DFT and CCSD(T) levels of theory. Neutral $[SiAu_4]$ is found to be a closed-shell singlet also with T_d symmetry and there is only a slight shortening of the Si–Au bond length (0.05 Å) compared to the anion. The relative energy difference between the two isomers is 0.47 eV for the neutral and 0.66 eV for the anion at the DFT level, and 0.39 eV for the neutral and 1.13 eV for the anion at the CCSD(T) level. Clearly, at the CCSD(T) level, the tetrahedral $[SiAu_4]^-$ is much more stable than the pyramidal isomer.

The geometry changes between the ground states of $[SiAu_n]^-$ and $[SiAu_n]$ (Figure 2) are consistent with the nature of the first PES band (X, Figure 1). The sharp threshold peaks in $[SiAu_2]^-$ and $[SiAu_4]^-$ and the broad band in $[SiAu_3]^-$ were all born out in the calculated structural changes from the anions to the neutrals. We further calculated the ADEs and VDEs for the ground state structures of $[SiAu_n]^-$ at both DFT and CCSD(T) levels of theory (Table 1). At the CCSD(T) level, the ADE of $[SiAu_2]^-$ and the VDEs of $[SiAu_2]^-$ and $[SiAu_3]^-$ are in quantitative agreement with the experimental values. The calculated ADE for $[SiAu_3]^-$ (2.93 eV) is much smaller than the experimentally estimated threshold value (3.22 eV). This difference is due to the large geometry change between the ground states of $[SiAu_3]^-$ and $[SiAu_3]$ such that there is negligible Franck–Condon factor for the 0–0 transition. In this case, the detachment threshold estimated from the PES spectra can only be viewed as an upper limit for the true ADE. For $[SiAu_4]^-$, the calculated VDE and ADE at both DFT and CCSD(T) agree well with the experimental values, but are off by about 0.16 eV in different directions at the two levels of theory (Table 1). We also calculated the vibrational frequencies for $[SiAu_4]$ at the B3LYP level and obtained an unscaled value of 127 cm^{-1} for the totally symmetric mode (see Supporting Information), in excellent agreement with the experimental value of 140 ± 30 cm^{-1}. To facilitate better comparison with the experiments we also simulated the PES spectra by using the time-dependent DFT method (Figure 3). Excellent overall agreement between the simulated spectra and the experimental data was observed,

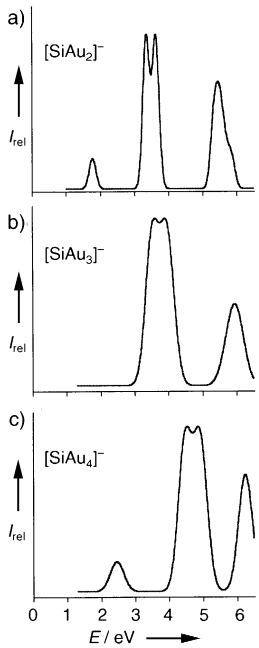

Figure 3. Simulated spectra of $[SiAu_n]^-$ ($n = 2$–4) by using TD-DFT. a) $[SiAu_2]^-$. b) $[SiAu_3]^-$. c) $[SiAu_4]^-$.

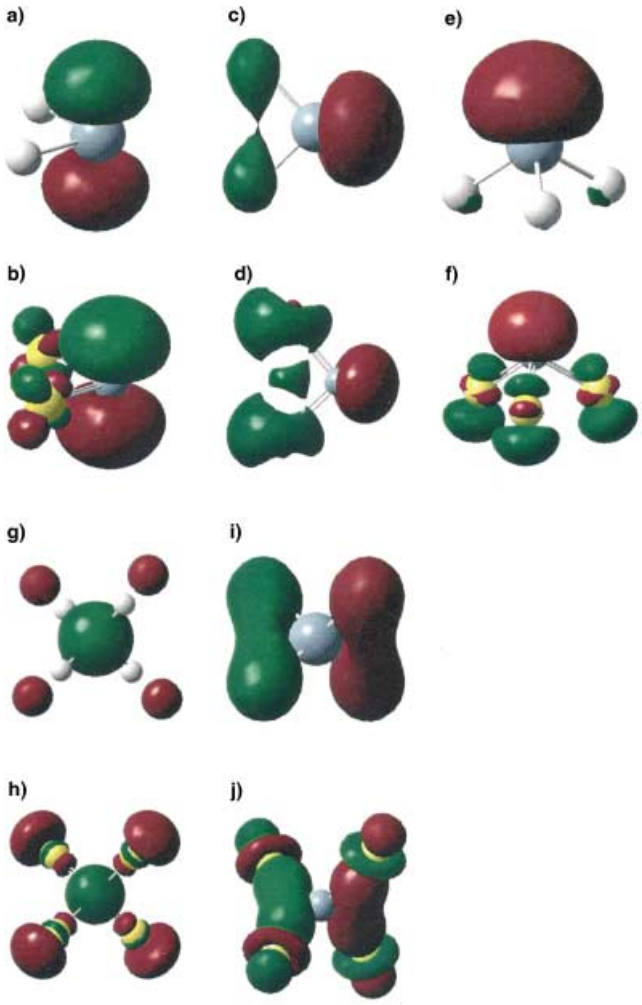

Figure 4. Comparison of the relevant frontier molecular orbitals between SiH_n and $[SiAu_n]$ ($n = 2$–4). a) The LUMO (b_1) of SiH_2. b) The LUMO (b_1) of $[SiAu_2]$. c) The HOMO (a_1) of SiH_2. d) The HOMO (a_1) of $[SiAu_2]$. e) The HOMO (a_1) of SiH_3. f) The HOMO (a_1) of $[SiAu_3]$. g) The LUMO (a_1) of SiH_4. h) The LUMO (a_1) of $[SiAu_4]$. i) one of the three Si–H bonding orbitals of SiH_4 (t_2). j) one of the three Si–Au bonding orbitals of $[SiAu_4]$ (t_2).

thus confirming the ground state structures for the $[SiAu_n]^-$ and $[SiAu_n]$ clusters.

We noted that the structures of the $[SiAu_n]$ clusters are nearly identical to the silicon hydride (SiH_n) molecules.[20] The geometry changes between the $[SiAu_n]^-$ ions and the $[SiAu_n]$ neutrals also exactly parallel those between SiH_n^- and SiH_n, that is, very little geometry change exists between SiH_2^- and SiH_2, and between SiH_4^- and SiH_4, whereas a large bond angle change occurs between SiH_3^- and SiH_3.[20] To further understand the chemical bonding in the Si–Au clusters, we analyzed the molecular orbitals (MOs) of $[SiAu_n]$ and compared them to those of the SiH_n counterparts (Figure 4 and Supporting Information). Except the sd hybridization in Au, the valence MOs that involve the Si–Au bonding in $SiAu_n$ ($n = 2$–4) are nearly identical to those of the corresponding SiH_n species. Like silylene, the HOMO of $SiAu_2$ (aurosilylene) is mainly a Si lone-pair (Figure 4d) and its LUMO is a pure silicon p orbital (Figure 4b). The HOMO of both $[SiAu_3]^-$ and SiH_3^- is a Si lone pair, which is one of the Si sp^3 hybrid MOs. Removal of an electron from this MO produces the doublet ground state for both $SiAu_3$ and SiH_3 and significantly flattens the neutral molecules in both cases. Similarly, the silane counterpart, $[SiAu_4]$, brings out sp^3 hybridization in silicon, analogous to that in SiH_4. The LUMO and the four Si–Au bonding orbitals are very similar to those in SiH_4 (Figure 4 and Supporting Information). Charge analysis by using the natural-bond-orbital theory revealed that the interaction between Si and Au in all $[SiAu_n]$ species is covalent with negligible charge transfer. This conclusion is consistent with a previous suggestion for a series of main-group XAu_n^{m+} (X = B–N, Al–S) species at the Hartree–Fock level.[21] Thus we observe a complete isolobal analogy between Au and H in the $[SiAu_n]$ series of molecules. This analogy is further supported by the similar electronegativity of gold (2.4) and hydrogen (2.2).

To evaluate the stability of the new $SiAu_n$ molecules, we calculated their atomization energies (at CCSD(T) level) and compared to the corresponding silicon hydrides:

$[SiAu_2]$ (C_{2v}, $^1A_1$) + 2 Au (^2S) → Si (^3P) $\Delta E = 5.82$ eV (134.2 kcal mol^{-1})

$[SiAu_3]$ (C_{3v}, $^2A_1$) + 3 Au (^2S) → Si (^3P) $\Delta E = 7.89$ eV (181.9 kcal mol^{-1})

$[SiAu_4]$ (T_d, $^1A_1$) + 4 Au (^2S) → Si (^3P) $\Delta E = 10.87$ eV (250.7 kcal mol^{-1})

$[SiH_2]$ (C_{2v}, $^1A_1$) + 2 H (^2S) → Si (^3P) $\Delta E = 6.52$ eV (150.4 kcal mol^{-1})

$[SiH_3]$ (C_{3v}, $^2A_1$) + 3 H (^2S) → Si (^3P) $\Delta E = 9.68$ eV (223.2 kcal mol^{-1})

$[SiH_4]$ (T_d, $^1A_1$) + 4 H (^2S) → Si (^3P) $\Delta E = 13.80$ eV (318.2 kcal mol^{-1})

The total atomization energies, as well as the single Si–Au bond energies in $[SiAu_2]$ (67.1 kcal mol^{-1}), $[SiAu_3]$ (60.6 kcal mol^{-1}), and $[SiAu_4]$ (62.7 kcal mol^{-1}), are amazingly similar to those in the corresponding Si–H molecules, SiH_2 (75.2 kcal mol^{-1}), SiH_3 (74.4 kcal mol^{-1}), and SiH_4 (79.6 kcal mol^{-1}).[22] These relatively high atomization energies and the strong Si–Au bonds reflect both the covalent nature of the Si–Au bonds and the high stability of the $[SiAu_n]$ silicon auride molecules.

Although Au and Si do not form any stable alloys, the Au–Si interfaces have been studied extensively owing to their importance in microelectronics. It has been shown that despite the fact that Au is a very stable and unreactive noble metal, it is very reactive on Si surfaces even at room temperature.[23] Several metastable Si–Au alloys, including a $[SiAu_4]$ phase, have been observed to form in the Si–Au interface.[24] However, the nature of the chemical interactions between Au and Si in the Si–Au interface is still not well understood.[25] The current finding of the Au/H analogy, the strong Si–Au covalent bonding, and the highly stable gaseous silicon auride species are consistent with the high reactivity of Au on Si surfaces and should provide further insight into the nature of the chemical interactions in the Si–Au interfaces. The new chemistry of Au in analogy to hydrogen may allow new auro analogues of hydride molecules to be designed. The extremely stable aurosilane, $[SiAu_4]$, may be synthesized in solution with stabilizing PR_3 ligands, opening a new area of Si–Au chemistry.

Experimental Section

Photoelectron spectroscopy: Details of the experimental apparatus have been published elsewhere.[26] Briefly, a compressed disk target made with Si–Au (1:10 atomic ratio) was used as the laser vaporization target with a helium carrier gas. Clusters from the source underwent a supersonic expansion and collimated with a skimmer. Negatively charged clusters were extracted from the cluster beam and were analyzed by a time-of-flight mass spectrometer. The $[SiAu_n]^-$ ($n = 2$–4) cluster anions of interest were mass-selected before photodetachment with one of the four photon energies: 532 nm (2.331 eV), 355 nm (3.496 eV), 266 nm (4.661 eV), and 193 nm (6.424 eV). Photoelectron spectra were measured by using a magnetic-bottle time-of-flight photoelectron analyzer with an electron kinetic energy resolution of $\Delta E_k/E_k \sim 2.5\%$. The spectrometer was calibrated with the known spectrum of Rh^-.

Theoretical calculations: The initial search of the most stable structures for $[SiAu_n]^-$ ($n = 2$–4) and vibrational frequency calculations were done using analytical gradient with the aug-cc-pVTZ basis set for silicon, and small-core pseudorelativistic Stuttgart effective core potential (ECP) and the corresponding basis set, augmented by two ($\alpha = 0.498$ and $\alpha = 1.461$) f-type polarization sets for gold.[27] All the lowest-energy structures were found to be minima. The lowest-energy structures were optimized by using the couple-cluster method [CCSD(T)] with the same basis set. Vertical-electron-detachment energies were calculated by using time-dependent density functional theory (TD-DFT) for neutral molecules, whereas ΔSCF method was used for closed-shell anions with hybrid (B3-LYP) functional at the CCSD(T) geometries. All the DFT and TD-DFT calculations were carried out by using Gaussian 03[28] and R(U)CCSD(T) calculations with the MOLPRO 2000.02 program.[29] Molecular orbitals were generated with GaussView. Gaussian 03 calculations were done at Washington State University Linux cluster and MOLPRO calculations were performed by using supercomputers at EMSL, Molecular Science Computing Facility of Pacific Northwest National Laboratory.

Received: December 22, 2003 [Z53602]
Published Online: March 11, 2004

Keywords: density functional calculations · gold · isolobal relationship · photoelectron spectroscopy · silicon

[1] P. Pyykkö, J. P. Desclaux, *Acc. Chem. Res.* **1979**, *12*, 276–281.
[2] P. Pyykkö, *Chem. Rev.* **1988**, *88*, 563–594.
[3] P. Schwerdtfeger, M. Dolg, W. H. E. Schwarz, G. A. Bowmaker, P. D. W. Boyd, *J. Chem. Phys.* **1989**, *91*, 1762–1774.
[4] P. Schwerdtfeger, *Chem. Phys. Lett.* **1991**, *183*, 457–463.
[5] P. Pyykkö, *Angew. Chem.* **2002**, *114*, 3723–3728; *Angew. Chem. Int. Ed.* **2002**, *41*, 3573–3578.
[6] H. Schwarz, *Angew. Chem.* **2003**, *115*, 4580–4593; *Angew. Chem. Int. Ed.* **2003**, *42*, 4442–4454.
[7] W. J. Peer, J. J. Lagowski, *J. Am. Chem. Soc.* **1978**, *100*, 6260–6261.
[8] A. V. Mudring, M. Jansen, J. Daniels, S. Kramer, M. Mehring, J. P. P. Ramalho, A. H. Romero, M. H. Parrinello, *Angew. Chem.* **2002**, *114*,128–132; *Angew. Chem. Int. Ed.* **2002**, *41*, 120–124.
[9] L. Gagliardi, *J. Am. Chem. Soc.* **2003**, *125*, 7504–7505.
[10] K. P. Hall, D. M. P. Mingos, *Prog. Inorg. Chem.* **1984**, *32*, 237–325.
[11] J. W. Lauher, K. Wald, *J. Am. Chem. Soc.* **1981**, *103*, 7648–7650.
[12] J. K. Burdett, O. Eisenstein, W. B. Schweizer, *Inorg. Chem.* **1994**, *33*, 3261–3268.
[13] F. Scherbaum, A. Grohmann, G. Müller, H. Schmidbaur, *Angew. Chem.* **1989**,*101*, 464–467; *Angew. Chem. Int. Ed. Engl.* **1989**, *28*, 463–466.
[14] A. Grohmann, H. Schmidbaur, *Nature* **1990**, *345*, 140–142.
[15] H. Schmidbaur, O. Steigelmann, *Z. Naturforsch. B* **1992**, *47*, 1721–1724.
[16] J. Li, P. Pyykkö, *Inorg. Chem.* **1993**, *32*, 2630–2634.
[17] H. Schmidbaur, F. P. Gabbai, A. Schier, J. Riede, *Organometallics* **1995**, *14*, 4969–4971.
[18] X. Li, B. Kiran, J. Li, H. J. Zhai, L. S. Wang, *Angew. Chem.* **2002**, *114*, 4980–4983; *Angew. Chem. Int. Ed.* **2002**, *41*, 4786–4789.
[19] J. Li, X. Li, H. J. Zhai, L. S. Wang, *Science* **2003**, *299*, 864–867.
[20] C. Pak, J. C. Rienstra-Kiracofe, H. F. Schaefer, *J. Phys. Chem. A* **2000**, *104*, 11232–11242.
[21] P. Pyykkö, Y. Zhao, *Chem. Phys. Lett.* **1991**, *177*, 103–106.
[22] The atomization energies obtained here for the Si–H species are in good agreement with a previous study: R. S. Grev, H. F. Schaefer, *J. Chem. Phys.* **1992**, *97*, 8389–8406.
[23] J. J. Yeh, J. Hwang, K. Bertness, D. J. Friedman, R. Cao, I. Lindau, *Phys. Rev. Lett.* **1993**, *70*, 3768–3771.
[24] Z. Ma. L. H. Allen, *Phys. Rev. B* **1993**, *48*, 15484–15487.
[25] J. Ivanco, H. Kobayashi, J. Almeida, G. Margaritondo, E. Pincik, *J. Appl. Phys.* **2001**, *90*, 345–350.
[26] L. S. Wang, H. Wu in *Advances in Metal and Semiconductor Clusters. IV. Cluster Materials* (Ed.: M. A. Duncan), JAI, Greenwich, CT, **1998**, pp. 299–343.
[27] J. M. L. Martin, A. Sundermann, *J. Chem. Phys.* **2001**, *114*, 3408–3420.
[28] Gaussian 03 (Revision B.04), M. J. Frisch,. G. W. Trucks, H. B. Schlegel, G. E. Scuseria, M. A. Robb, J. R. Cheeseman, J. A. Montgomery, Jr., T. Vreven, K. N. Kudin, J. C. Burant, J. M. Millam, S. S. Iyengar, J. Tomasi, V. Barone, B. Mennucci, M. Cossi, G. Scalmani, N. Rega, G. A. Petersson, H. Nakatsuji, M. Hada, M. Ehara, K. Toyota, R. Fukuda, J. Hasegawa, M. Ishida, T. Nakajima, Y. Honda, O. Kitao, H. Nakai, M. Klene, X. Li, J. E. Knox, H. P. Hratchian, J. B. Cross, C. Adamo, J. Jaramillo, R. Gomperts, R. E. Stratmann, O. Yazyev, A. J. Austin, R. Cammi,

C. Pomelli, J. W. Ochterski, P. Y. Ayala, K. Morokuma, G. A. Voth, P. Salvador, J. J. Dannenberg, V. G. Zakrzewski, S. Dapprich, A. D. Daniels, M. C. Strain, O. Farkas, D. K. Malick, A. D. Rabuck, K. Raghavachari, J. B. Foresman, J. V. Ortiz, Q. Cui, A. G. Baboul, S. Clifford, J. Cioslowski, B. B. Stefanov, G. Liu, A. Liashenko, P. Piskorz, I. Komaromi, R. L. Martin, D. J. Fox, T. Keith, M. A. Al-Laham, C. Y. Peng, A. Nanayakkara, M. Challacombe, P. M. W. Gill, B. Johnson, W. Chen, M. W. Wong, C. Gonzalez, J. A. Pople, Gaussian, Inc., Pittsburgh, PA, **2003**.

[29] MOLPRO a package of ab initio programs designed by H. J. Werner and P. J. Knowles, version 2002.6, R. D. Amos, A. Bernhardsson, A. Berning, P. Celani, D. L. Cooper, M. J. O. Deegan, A. J. Dobbyn, F. Eckert, C. Hampel, G. Hetzer, P. J. Knowles, T. Korona, F. Lindh, A. W. Lloyd, S. J. McNicholas, F. R. Manby, W. Meyer, M. E. Mura, A. Nicklass, P. Palmieri, R. Pitzer, G. Gauhut, M. Schultz, U. Schumann, H. Stoll, A. J. Stone, R. Tarroni, T. Thorsteinsson, H. J. Werner.

